CARBON 82 (2015) 353–359

Available at www.sciencedirect.com

ScienceDirect

journal homepage: www.elsevier.com/locate/carbon

Preparation and characterization of graphene paper for electromagnetic interference shielding

Lu Zhang [a], Noe T. Alvarez [a], Meixi Zhang [a], Mark Haase [a], Rachit Malik [a], David Mast [b], Vesselin Shanov [a,*]

[a] Nanoworld Laboratories, Department of Chemical and Materials Engineering, University of Cincinnati, Cincinnati, OH 45221-0072, USA
[b] Department of Physics, University of Cincinnati, Cincinnati, OH 45221-0072, USA

ARTICLE INFO

Article history:
Received 10 July 2014
Accepted 24 October 2014
Available online 30 October 2014

ABSTRACT

Syntheses of multifunctional structures, both in two-dimensional and three-dimensional space, are essential for advanced graphene applications. A variety of graphene-based materials has been reported in recent years, but combining their excellent mechanical and electrical properties in a bulk form has not been entirely achieved. Here, we report the creation of novel graphene structures such as graphene pellet and graphene paper. Graphene pellet is synthesized by chemical vapor deposition (CVD), using inexpensive nickel powder as a catalyst. Graphene pellet can be further processed into a graphene paper by pressing. The latter possesses high electrical conductivity of up to 1136 ± 32 S cm^{-1} and exhibits a breaking stress at 22 ± 1.4 MPa. Further, this paper-like material with thickness of 50 μm revealed 60 dB electromagnetic interference (EMI) shielding effectiveness.

1. Introduction

The proliferation of electronic devices in recent decades has greatly increased the potential for EMI. Electromagnetic radiation at high frequencies can easily interfere with electronic devices and is also harmful to human health. Consequently, there is a significant interest in the development of materials for EMI shielding. Generally, materials with good electrical conductivity show good shielding performance in reducing the energy of penetrating electromagnetic radiations. For example, metals with good electrical conductivity (e.g., copper, nickel, aluminum) show good performance for EMI shielding [1]. However, in many applications (such as aerospace electronics), the material for EMI shielding besides of being effective, needs to be lightweight and flexible, especially in applications of flexible electronics, aircrafts and automobiles. Thus the density and flexibility of shielding materials are usually evaluated in EMI shielding applications, making carbon materials [2–5] competitive with metals.

For example, research suggests that graphene has the potential to be an excellent EMI shielding material with up to 500 dB cm^3 g^{-1} specific EMI shielding effectiveness when incorporated in a PMDS matrix [2]. Flexible graphite with an EMI shielding effectiveness of 130 dB was also reported [6]. However, the thickness is a major factor that needs to be considered when comparing the SE of different shielding materials. According to the plane-wave theory [7], larger thickness of shielding materials will yield higher shielding effectiveness in dB. This dependence is not linear, since both reflection and absorption are involved. Thus it is worth to mention that the thicknesses of the reported carbon shielding materials [2–6] are three orders higher compared to shield of copper film [1] which limit their applications as thin, protective layers for EMI shielding of sensitive instruments. The relative large

* Corresponding author.
http://dx.doi.org/10.1016/j.carbon.2014.10.080

thickness of these carbon based shielding materials is due to the poor mechanical properties that call for polymer coating, which enlarges the thickness and adds additional processing steps. This polymer coating reduces the carbon filler fraction in the carbon/polymer shield resulting in a low electrical conductivity of the composite material. This explains the absolute shielding effectiveness of these carbon/polymer composite materials [2–5,8–15] is usually low compared to copper or nickel.

One approach to increase the electrical conductivity of carbon/polymer EMI shielding materials is to increase the carbon filler content, thus making paper-like pristine graphene materials [16–19] promising for new shielding applications especially in the aerospace industry where the weight matters. This EMI shielding application of graphene paper is related to its low density, excellent flexibility and extraordinary electrical properties of graphene materials [20–23]. Graphene paper [16] prepared by using graphene oxide (GO) as a template for synthesis and processing showed good mechanical properties with a breaking stress at 120 MPa. However, the poor conductivity of GO – resulting from the introduction of oxygen and surface defects during preparation – limits its applications [19]. Recently, highly electrical and thermal conductive GO paper prepared by direct evaporation demonstrated a EMI shielding effectiveness of 20 dB was reported [24], but GO paper prepared by similar method usually shows relatively high density [16], which limits its application as a light EMI shielding materials. Graphene made through CVD has an overall high quality. By using this method, graphene paper [18] with good electrical conductivity has been achieved by filtration of the CVD graphene foams [25], but the poor mechanical strength of this material requires supporting substrate and expensive catalyst template – nickel foam – which may be a barrier for industrial scale up.

Here, we report a novel, freestanding graphene paper prepared by CVD synthesis of 3D graphene pellets, extracting the Ni catalyst and pressing the remaining structure to form a paper-like material [26].

2. Experimental

2.1. Sample preparation

2.1.1. Fabrication of graphene pellet

Nickel powder (Alfa Aesar) of 2–3 μm average particle size and 0.68 $m^2 g^{-1}$ in specific surface area was pelletized into 6.4 cm diameter pellets using a compression machine (Carver, 973214A). The applied force was ~10 MPa, and varied for different pellet thicknesses. The nickel pellet was placed on a quartz platform inside a quartz tube for growing of graphene by CVD. The nickel pellet was heated up to 1000 °C in a tube furnace (FirstNano, ET1000) under Ar (1000 sccm). Hydrogen (325 sccm) was then introduced for 15 min, to reduce any metal catalyst oxide. Then, CH_4 was introduced for 5 min. Various hydrocarbon flow rates were tested (12, 15, 18, 25 and 28 sccm, corresponding to concentrations of 0.9, 1.1, 1.3, 1.9 and 2.1 vol%, respectively). The pellet was then cooled to room temperature with a rate of ~100 °C min^{-1} under Ar (1,000 sccm) and H_2 (325 sccm). The nickel pellet shrank ~30% in all dimensions after CVD. The final 3D graphene structure in the form of pellet was produced by etching out nickel from the graphene/nickel pellet with HCl (3 M) at 80 °C for 10 h. The obtained graphene pellet was washed with water to remove residual acid and dried at room temperature.

2.1.2. Fabrication of graphene paper

Graphene paper was obtained by compressing the graphene pellet with a press between 2 flat steel plates. Different thicknesses of graphene paper can be fabricated by changing the compression load (Table S1).

2.2. Analysis

2.2.1. Microscopic characterization

SEM (FEI XL30, 15 kV), Raman spectroscopy (Renishaw inVia, excited by a 514 nm He–Ne laser with a laser spot size of ~1 μm^2) and TEM (FEI CM20, 300 kV) were used to characterize the of graphene paper. For the SEM tests, the sample did not need any additional conductive coating due to the high electrical conductivity of the graphene paper. The preparation of the TEM sample included ultrasound dispersion of the graphene paper in ethanol for 30 min. A drop of the obtained suspension was applied to a TEM grid and dried for observation.

2.2.2. Electrical and mechanical measurements

A four-point probe (Jandel RM3000) was used for electrical measurement of the samples. Four terminals of the probe were slightly compressed on the surface of a graphene paper with a dimension of 1 cm × 1 cm. The electrical conductivity was calculated based on the thickness of graphene paper, which was measured by a micrometer. The thickness measurement of graphene paper showed a typical error with the range of ±3%. The strength of the graphene paper was evaluated by employing a mechanical testing system (Instron 5948). The test samples were cut into 10 mm × 1 mm coupons by laser and gripped by two pneumatic clips. The test was conducted with a strain rate of 0.5 mm min^{-1}.

2.2.3. EMI shielding effectiveness measurement

The EMI shielding effectiveness was measured in the X-band frequency ranging from 8 to 12 GHz using a vector network analyzer (Agilent N5222A) and two waveguide-to-coaxial adapters with dimensions of 4 cm × 4 cm and an electromagnetic wave channel of 2 cm × 1 cm. The scattering parameter (S_{21}) between the two waveguide-to-coaxial adapters was determined by the vector network analyzer. The samples were cut into 2.5 cm × 1.3 cm coupons with thickness ~50 μm and placed into the narrow waveguide gap created for the measurement.

3. Results and discussion

Fig. 1a illustrates the processing of graphene paper, in which nickel powder catalyst was pelletized by applying ~10 MPa pressure to a known mass of the metal confined in a piston-cylinder mold. The metal catalyst powder was sintered into an interconnected foam-like structure under the applied high temperature inside the CVD reactor (Fig. S1a and b). Graphene

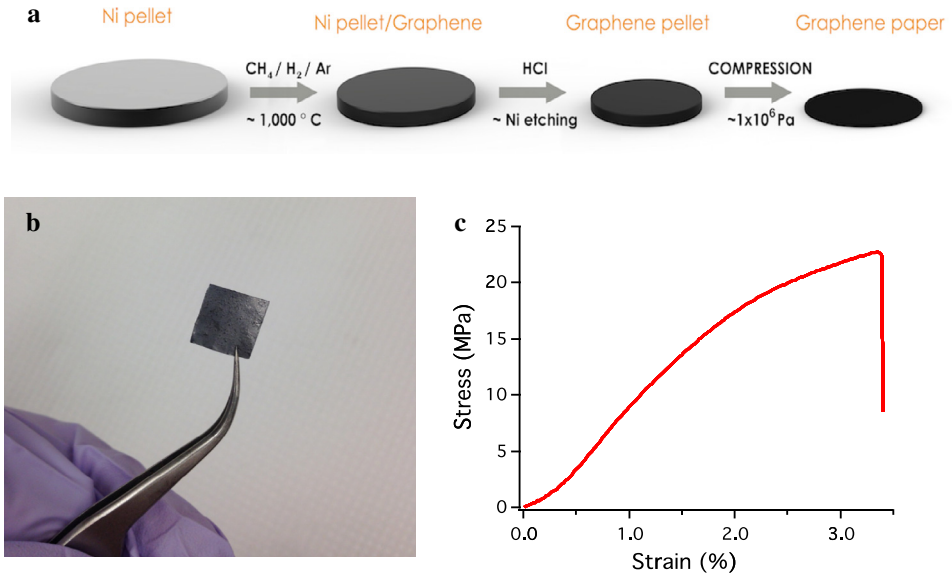

Fig. 1 – Illustration showing the CVD synthesis of graphene pellet and its processing into graphene paper: (a) Synthesis steps of making graphene pellet (3 cm in diameter) and processing it into graphene paper. (b) Photo of graphene paper (1 cm × 1 cm). (c) Typical tensile stress strain curve of graphene paper. The graphene paper here was prepared from 3D graphene pellet synthesized with 1.9 vol% CH_4 in CVD. (A colour version of this figure can be viewed online.)

was then synthesized from this pellet by introducing methane which resulted in forming of a monolith 3D graphene network of interconnected flakes, as displayed in Fig. S1c and d. After synthesis, the nickel template was etched out by immersion in HCl acid, leaving a freestanding three-dimensional and porous graphene pellet (Fig. S1e and S2c). The maximum graphene pellet dimensions in our work were 4 cm by 2 cm. Typically, the graphene pellet prepared with 25 sccm methane in the CVD gas phase has a density of 0.15 g cm^{-3} and exhibits good mechanical strength compared to nickel foam reported previously [25]. The latter required polymer reinforcement to maintain its structural integrity during the nickel etching. Our polymer-free process for preparing the graphene pellet benefits the electrical conductivity of graphene and enables making a 3D structure consisted of 100% graphene. After rinsing the acid with DI water and drying, the obtained graphene retained a 3D structure, albeit with reduced dimensions compared to the nickel pellet. Graphene pellet can be further processed to a graphene paper by pressing it between 2 flat steel plates.

The obtained graphene paper is quite flexible, can be folded at 180° and recover its initial shape upon release of the folding force (Fig. 1b and Fig. S2). Besides flexibility, the graphene paper also shows high mechanical strength. The Stress–Strain curve shows a breaking stress at 22 ± 1.4 MPa for graphene paper made with 1.9 vol% CH_4 (Fig. 1c). This stress value is higher than the same parameter of graphene foam reinforced with a PMMA coating [25]. The employed method of manufacturing graphene paper in our experiment avoids use of polymer support which contributes to the increased electrical conductivity of this material.

The morphology of graphene paper was studied by scanning electron microscopy (SEM) (Fig. 2a and b), which shows the wrinkles and ripples of the graphene flakes. This morphology may be caused by the difference between the thermal expansion coefficients of nickel and graphene [27]. Gaps were created among graphene flakes when the nickel powders were extracted from the Ni template leaving multiple graphene flakes in random 3D positions. Due to the good mechanical strength, the cross section thickness and morphology of the graphene paper can also be revealed by SEM (Fig. 2b). This image shows that the graphene paper is composed of highly compacted flakes. It also reveals the thickness of the tested paper which is measured as ~35 μm. The high-magnification transmission electron microscopy (TEM) image (Fig. 2c) displays a four-layer structure of the studied graphene flake with a distance of 0.32 nm between each layer. The inserted diffraction pattern in Fig. 2c indicates the graphene flakes within the paper reveal a multilayer structure, which is in agreement with the TEM image. Unlike graphite, which has a broad 2D peak at 2730 cm^{-1} in its Raman spectrum (Fig. 2d), the graphene paper in our work has a sharp 2D peak at 2707 cm^{-1} indicating fewer layers of graphene [28]. The suppressed D peak in the Raman spectrum of the graphene paper suggests high graphene quality.

The obtained graphene paper has a relatively low density, ranging from 0.6 up to 1.1 g cm^{-3}. This quality was inherited from the low density of the graphene pellet and relatively porous structure created by etching of the nickel catalyst. The low densities of the graphene paper and graphene pellet are also resulted from the porous structure created by the compressed nickel particles. The graphene paper density can be controlled either chemically, by adjusting the methane concentration during synthesis (Fig. 3a), or physically, by varying the force used to flatten the graphene pellet into graphene paper (Table S1). Using a chemical control, the higher carbon precursor concentration results in a denser and better-interconnected graphene structure. In addition, the carbon

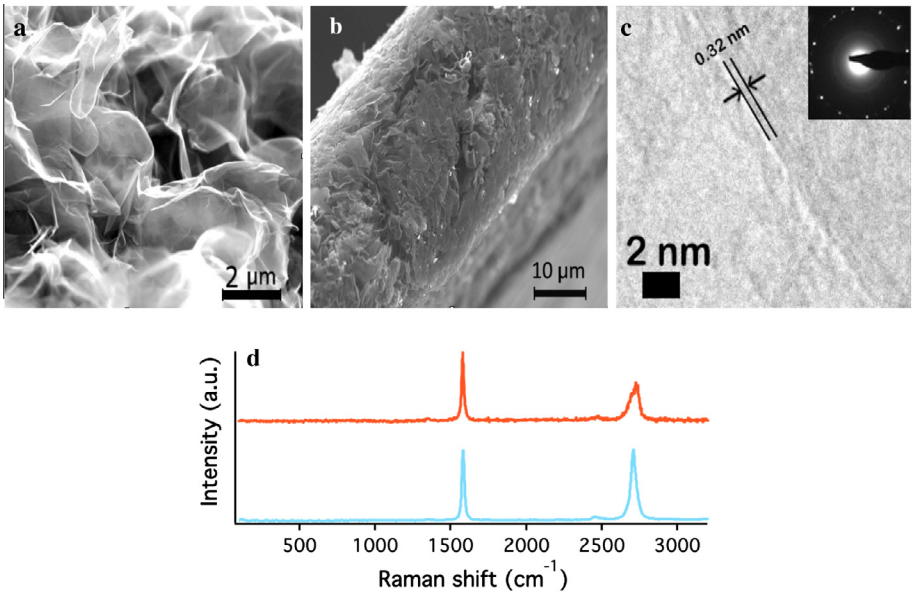

Fig. 2 – Characterization of graphene paper: (a) High magnification SEM image of the cross section of graphene paper. (b) Low magnification SEM image of the cross section of graphene paper, indicating a thickness of ~35 μm. (c) TEM image of graphene paper, showing a four layer structure of graphene flake with a distance of 0.32 nm between each layer. The inset is the electron diffraction pattern indicating the multilayer structure of the observed graphene flakes. (d) Raman spectrum of pure graphite powder (upper/red) and graphene paper (bottom/blue). The graphene paper was prepared with 1.9 vol% CH_4 during the CVD process. (A colour version of this figure can be viewed online.)

adsorption capacity of the catalyst during the CVD process may also play a role. Since the bulk density of graphene paper varies significantly when changing the pressing load, the areal density is used here to investigate the independent contribution of CH_4 to the density of graphene structure (Fig. 3a). With the same compression load, higher areal density graphene paper can be obtained by increasing the CH_4 during CVD process. Using physical control, higher mechanical compression leaves smaller voids between the graphene flakes, thus increasing the density dramatically (Table S1). Further, the increased density improves the electron transfer within the whole graphene structure by reducing the inter-flake resistance.

Varying the density, either by adjusting it chemically or physically, significantly affects the electrical conductivity of the graphene paper. For example, graphene paper produced with 0.9 vol% CH_4 concentration has a conductivity of 233 S cm^{-1} and increases up to 680 S cm^{-1} when rising CH_4 to 1.9 vol% (Fig. 3b). However, once CH_4 concentration exceeds a certain threshold, further increasing the concentration will lead to amorphous carbon accumulation, which decreases the electrical conductivity of the graphene paper. We found that this threshold is around 2.0 vol% of CH_4 at ambient pressure in the CVD reactor and further increase to 2.1 vol% CH_4 declined the conductivity value down to 617 S cm^{-1}. It was also noted that carbon deposits heavily on CVD furnace tube if the methane concentration exceeds this critical value.

The thickness of graphene paper is determined in part by the compressive load. We found a load of 0.1 MPa produces a 58 μm thick paper, while 1.1 MPa load yields a 32 μm thickness, as shown in (Table S1). Consequently, the electrical conductivity changes from 680 S cm^{-1} (with a 0.1 MPa pressing force) to 1,136 S cm^{-1} (with a 1.1 MPa pressing force), which corresponds to an increase up to 67%, as shown in Fig. 3c. This value is nearly three times higher than the published data for annealed GO paper, and to our knowledge is one of the highest conductivity values reported so far for paper-like graphene structures [16–19] (Table S2). It is worth mentioning that further compression of the graphene paper did not lead to the reduced thickness.

EMI shielding effectiveness is defined as the reflection plus absorption energy of electromagnetic radiation caused by a shielding material. It can be calculated in dB by taking the logarithmic ratio of incoming power and transmitted power of an electromagnetic wave. The specific EMI shielding effectiveness is obtained by dividing the EMI shielding effectiveness by the material's density and is often given in dB cm^3 g^{-1}. This parameter is frequently used for applications in which density is an important design factor.

For our study, EMI waveguides used to isolate the measurement environment from external radio frequency interferences were employed, as displayed in Fig. S3. The EMI shielding effectiveness (SE) is calculated based on the equation: $SE = -10 \log_{10} |T|$ (dB), $T = |S_{21}|^2$, in which T refers to the transmittance of the shield and S_{21} refers to the scattering parameter. Since the graphene paper in our work was highly conductive and with low density, high EMI shielding effectiveness and high specific EMI shielding effectiveness were expected. Graphene paper with thickness of ~50 μm, fabricated by using 0.9 vol% CH_4 concentration showed a shielding effectiveness of ~40 dB (Fig. 4a-i) and this value increased up to ~60 dB when the methane concentration was raised to 1.1 vol% (Fig. 4b-ii) and 1.9 vol% (Fig. 4a-iii). To achieve further improvements of the EMI shielding effectiveness, two

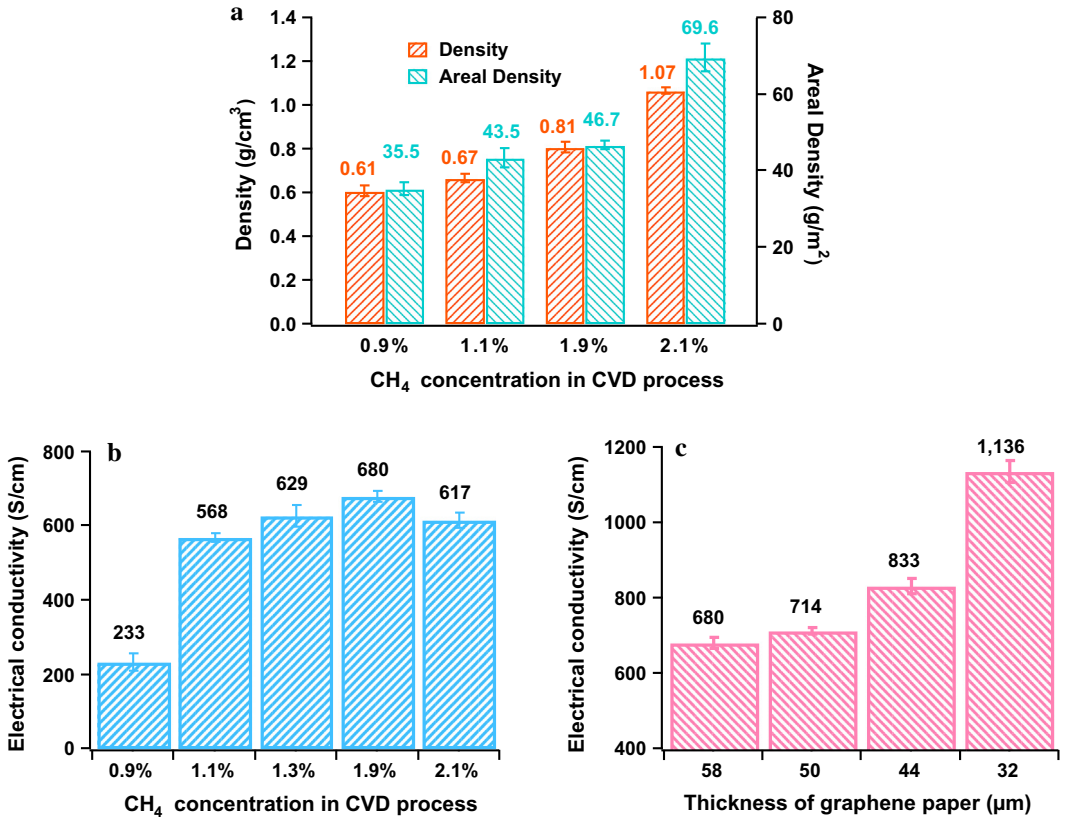

Fig. 3 – Density and electrical conductivity of graphene paper: (a) Density and areal density of graphene paper as a function of methane concentration used during the CVD process. The error bars represent the standard deviations calculated based on 3 specimens for each sample. The thickness of all the samples used to calculate the density was ~60 μm. (b) Electrical conductivity of the graphene paper prepared by using different CH_4 concentrations. The error bars represent the standard deviations which were calculated based on 3 specimens for each sample. (c) Electrical conductivity of 1.9 vol% CH_4 graphene paper as a function of the paper thickness. (A colour version of this figure can be viewed online.)

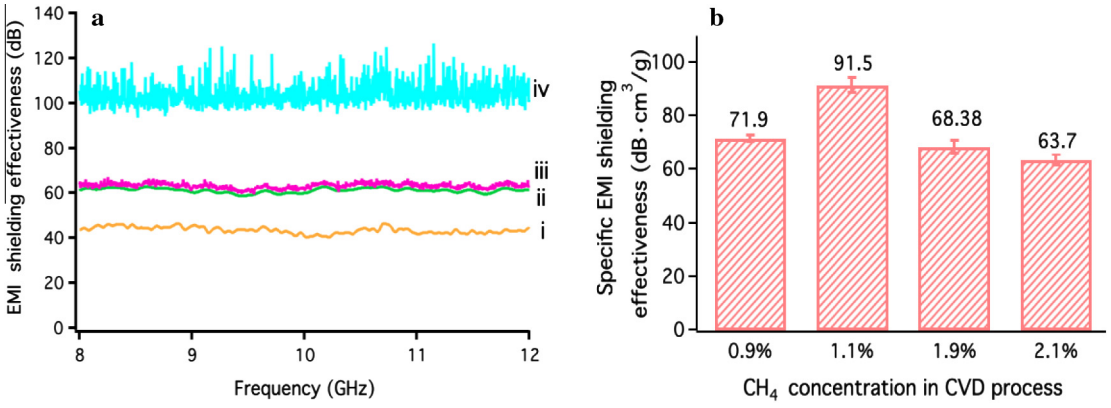

Fig. 4 – EMI shielding effectiveness of graphene paper: (a) Shielding effectiveness of graphene paper fabricated with (i) 0.9 vol% CH_4; (ii) 1.1 vol% CH_4; (iii) 1.9 vol% CH_4; (iv) two stacked on top of each other paper specimens both produced with 1.9 vol% CH_4. (b) Specific shielding effectiveness of graphene paper manufactured with different CH_4 concentrations. The error bars represent the standard deviations which were calculated based on 3 specimens for each methane concentration. The shielding effectiveness was calculated by averaging the data from 8 GHz to 12 GHz (X band). (A colour version of this figure can be viewed online.)

~50 μm thick graphene papers synthesized with 1.9 vol% CH_4 concentration were stacked together on top of each other and used as a test material during an additional EMI shielding effectiveness experiment. The resulting total thickness of the created graphene shield was about 100 μm. The obtained shielding effectiveness showed a value higher than 100 dB (Fig. 4a-iv). This value can be hardly achieved by any other carbon nanostructured material with similar thickness without using of metal coatings. The latter will increase the areal density of the shielding material, which may not be favorable for aerospace applications. A comparison between graphene paper prepared in this work and other carbon and metal materials reported in the literature is shown in Table S3. The data displayed there suggests that graphene paper made as described here can be a strong candidate for replacing metals in EMI shielding applications. When prepared from 1.1 vol% CH_4 concentration, the graphene paper revealed a specific EMI shielding effectiveness of 91.5 dB $cm^3 g^{-1}$ (Fig. 4b), which is almost one order higher than the one reported for copper and nickel. Graphene paper manufactured with 1.9 vol% CH_4 shows also a good conductivity and EMI shielding effectiveness. However, due to its higher density compared to the 1.1 vol% CH_4 sample, it reveals specific shielding effectiveness of 68.38 dB $cm^3 g^{-1}$, which is slightly lower than 1.1 vol% CH_4 sample. When CH_4 concentration is raised above approximately 2.0 vol%, the specific shielding effectiveness decreases, due to the resulting drop in conductivity and increase in density.

4. Conclusion

We have developed a polymer free process for synthesis of three dimensional graphene structures and graphene paper, consisted of 100% graphene, using nickel pellet as a catalyst template during the CVD synthesis, followed by acid extraction the catalyst and pressing the remaining structure. The 3D graphene and the related graphene paper are mechanically robust. The paper shows high electrical conductivity, attributed to the good quality of the individual graphene flakes and their connectivity within the three-dimensional structure. The obtained graphene paper also reveals excellent EMI shielding effectiveness and specific EMI shielding effectiveness, while maintaining thickness below 100 μm. The synthesis and processing scale up of our 3D graphene paper material is feasible because of the available commercial CVD reactors that can accommodate samples with diameter of 100 cm and greater. Preparing of Ni pellets by pressing large size templates is possible with industrial molds, which are standard tools in many powder metallurgy sites and can manufacture samples with dimensions of 100×100 cm and above.

The obtained graphene paper has a great potential for a wide range of application including, but not limited to EMI shielding, sensors, batteries and supercapacitors.

Acknowledgments

This work was funded by the National Science Foundation through the following grants: CMMI-0727250; SNM-1120382; ERC-0812348; and by a DURIP-ONR grant. The support of the listed Government agencies is gratefully acknowledged.

Appendix A. Supplementary data

Supplementary data associated with this article can be found, in the online version, at http://dx.doi.org/10.1016/j.carbon.2014.10.080.

REFERENCES

[1] Shui XP, Chung DDL. Nickel filament polymer-matrix composites with low surface impedance and high electromagnetic interference shielding effectiveness. J Electron Mater 1997;26:928–34.
[2] Chen Z, Xu C, Ma C, Ren W, Cheng H-M. Lightweight and flexible graphene foam composites for high-performance electromagnetic interference shielding. Adv Mater 2013;25:1296–300.
[3] Fletcher A, Gupta MC, Dudley KL, Vedeler E. Elastomer foam nanocomposites for electromagnetic dissipation and shielding applications. Compos Sci Technol 2010;70:953–8.
[4] Zhang H-B, Yan Q, Zheng W-G, He Z, Yu Z-Z. Tough graphene–polymer microcellular foams for electromagnetic interference shielding. ACS Appl Mater Interfaces 2011;3:918–24.
[5] Yang Y, Gupta MC, Dudley KL, Lawrence RW. Novel carbon nanotube–polystyrene foam composites for electromagnetic interference shielding. Nano Lett 2005;5:2131–4.
[6] Luo X, Chung DDL. Electromagnetic interference shielding reaching 130 dB using flexible graphite. MRS Proceedings, Cambridge Univ Press; p. 235.
[7] Kaynak A. Electromagnetic shielding effectiveness of galvanostatically synthesized conducting polypyrrole films in the 300–2000 MHz frequency range. Mater Res Bull 1996;31:845–60.
[8] Chung DDL. Electromagnetic interference shielding effectiveness of carbon materials. Carbon 2001;39:279–85.
[9] Geetha S, Satheesh Kumar KK, Rao CRK, Vijayan M, Trivedi DC. EMI shielding: methods and materials – A review. J App Poly Sci 2009;112:2073–86.
[10] Eswaraiah V, Sankaranarayanan V, Ramaprabhu S. Functionalized graphene–PVDF foam composites for EMI shielding. Macromol Mater Eng 2011;296:894–8.
[11] Thomassin J-M, Pagnoulle C, Bednarz L, Huynen I, Jerome R, Detrembleur C. Foams of polycaprolactone/MWNT nanocomposites for efficient EMI reduction. J Mate Chem 2008;18:792–6.
[12] Li N, Huang Y, Du F, He X, Lin X, Gao H, et al. Electromagnetic interference (EMI) shielding of single-walled carbon nanotube epoxy composites. Nano Lett 2006;6:1141–5.
[13] Liang J, Wang Y, Huang Y, Ma Y, Liu Z, Cai J, et al. Electromagnetic interference shielding of graphene/epoxy composites. Carbon 2009;47:922–5.
[14] Liu Z, Bai G, Huang Y, Ma Y, Du F, Li F, et al. Reflection and absorption contributions to the electromagnetic interference shielding of single-walled carbon nanotube/polyurethane composites. Carbon 2007;45:821–7.
[15] Wang L-L, Tay B-K, See K-Y, Sun Z, Tan L-K, Lua D. Electromagnetic interference shielding effectiveness of carbon-based materials prepared by screen printing. Carbon 2009;47:1905–10.

[16] Dikin DA, Stankovich S, Zimney EJ, Piner RD, Dommett GHB, Evmenenko G, et al. Preparation and characterization of graphene oxide paper. Nature 2007;448:457–60.
[17] Chen H, Müller MB, Gilmore KJ, Wallace GG, Li D. Mechanically strong, electrically conductive, and biocompatible graphene paper. Adv Mat 2008;20(18):3557–61.
[18] Chen J, Bi H, Sun S, Tang Y, Zhao W, Lin T, et al. Highly conductive and flexible paper of 1D silver-nanowire-doped graphene. ACS Appl Mater Interfaces 2013;5:1408–13.
[19] Stankovich S, Dikin DA, Piner RD, Kohlhaas KA, Kleinhammes A, Jia Y, et al. Synthesis of graphene-based nanosheets via chemical reduction of exfoliated graphite oxide. Carbon 2007;45:1558–65.
[20] Novoselov KS, Geim AK, Morozov SV, Jiang D, Zhang Y, Dubonos SV, et al. Electric field effect in atomically thin carbon films. Science 2004;306:666–9.
[21] Avouris P, Chen Z, Perebeinos V. Carbon-based electronics. Nat Nanotechnol 2007;2:605–15.
[22] Kotov NA. Materials science: carbon sheet solutions. Nature 2006;442:254–5.
[23] Gómez-Navarro C, Burghard M, Kern K. Elastic properties of chemically derived single graphene sheets. Nano Lett 2008;8:2045–9.
[24] Shen B, Zhai W, Zheng W. Ultrathin flexible graphene film: an excellent thermal conducting material with efficient EMI shielding. Adv Funct Mater 2014;24:4542–8.
[25] Chen Z, Ren W, Gao L, Liu B, Pei S, Cheng H-M. Three-dimensional flexible and conductive interconnected graphene networks grown by chemical vapour deposition. Nat Mater 2011;10:424–8.
[26] Shanov V, Zhang L, Alvarez N, Zhang M, Haase M, Mast D, Malik R. A graphene paper and a process for making of graphene paper. U.S. Provisional Patent Application 61/971,237, filed March 27, (2014).
[27] Chae SJ, Güneş F, Kim KK, Kim ES, Han GH, Kim SM, et al. Synthesis of large-area graphene layers on poly-nickel substrate by chemical vapor deposition: wrinkle formation. Adv Mater 2009;21:2328–33.
[28] Ferrari AC, Meyer JC, Scardaci V, Casiraghi C, Lazzeri M, Mauri F, et al. Raman spectrum of graphene and graphene layers. Phys Rev Lett 2006;97:187401.